

Investigating Ground Deformation at Krakatoa Volcano Derived from InSAR and Local Seismic Tomography Analysis

Lucky FAKHRIADI, Dzauqi ARANI, Mutiara JAMILAH, Arliandy P ARBAD and Daffa ARROFI, Indonesia

ABSTRACT

One of the deadliest volcanic eruption in world history is the Krakatoa eruption on August 27, 1883. The eruption created caldera-forming which destroyed two-thirds of the Krakatoa volcanic island in the Sunda Strait resulting in the remaining of three small islands later known as the Krakatoa complex. The eruptive periods were between 1-8 years and on average between 2-4 years earlier. Eruptions in the center of Krakatoa complex have produced a new volcano named Anak Krakatoa, which is continuously building its body through eruptions until now. Previous records indicate that Mt. Krakatoa is dominated by Strombolian eruptions with relatively mild explosives at discrete but fairly regular intervals of seconds to minutes. Eruptions were characterized by Strombolian activities of pyroclastic and lava flows. We observed the ground deformation of Anak Krakatoa Volcano by interfering PALSAR-2 data from 2014 to 2015. A map of the averaged LOS velocity identifies actively the deforming volcanoes related to subsurface magma or hydrothermal movements. Another most interesting feature of this study is a zone of high V_p/V_s ratio beneath the Krakatoa complex. The comparison result of the technique shows a complex pattern of ground deformation. Inflation up to 3 cm, together with subsidence around the crater. The southwest side of the volcanic cone has been subsided by 10 cm, whereas the northeast side of the cone uplifted 8 cm in almost a year and causing significant volcano-wide subsidence and initiating a new interruption deformation cycle. We assumed the magma reservoirs beneath the Krakatoa complex as sponge-structured volumes that may quickly change the body of volcano rapidly through the volcanic system of Krakatoa.

Keywords : Krakatoa, Volcano, Monitoring, ,Eruption, Radar

Investigating Ground Deformation at Krakatoa Volcano Derived from InSAR and Local Seismic Tomography Analysis

Lucky FAKHRIADI, Dzauqi ARANI, Mutiara JAMILAH, Arliandy P ARBAD and Daffa ARROFI, Indonesia

1. INTRODUCTION

One of the most deadliest the catastrophic volcanic eruption in world history is the Krakatoa eruption on August 27, 1883. The eruption was creating caldera-forming which destroyed two-thirds of the Krakatoa volcanic island in the Sunda Strait resulting in the remaining three small islands later known as the Krakatoa complex. The eruptive periods recorded between 1-8 years and on average between 2-4 years earlier.

Eruptions in the center of Krakatoa complex have produced a new volcano named Anak Krakatoa, which continuously builds its body through eruptions until now. Previous records indicate that Mt. Krakatoa is dominated by Strombolian eruptions with, relatively mildly explosive ones at discrete but fairly regular intervals of seconds to minutes. Case studies conducted in regions such as figure 1



Figure 1. Area Study
(Google Maps, 2020)

2. METHOD

2.1 Data

For analysing the interferometric SAR we used SAR data derived from PALSAR-2 sensor and Images which L-band frequency characteristic on board from Advanced Land Observing Satellite (ALOS) with active microwave sensor to achieve cloud-free and day-and-night land observation. The dataset is composed of 2 SAR images, collected from 22 Sept 2014 and 9 Feb 2015 (Descending passes, HH polarization). In total, we selected 730 events with 3128 P- and 2050 S-phases. This dataset includes some deep focused events with depths of about 15 Km. The input data for the code are station coordinates and S-wave band arrival times of local earthquakes. The code can start performing calculations without using any a priori information on the sources. In this case, searching for the event locations starts from the center of the network or from the station with minimal travel time.

Landsat 8 was developed as a collaboration between NASA and the U.S. Geological Survey (USGS). NASA led the design, construction, launch, and on-orbit calibration phases, during which time the satellite was called the Landsat Data Continuity Mission (LDCM). On May 30, 2013, USGS took over routine operations and the satellite became Landsat 8. USGS leads post-launch calibration activities, satellite operations, data product generation, and data archiving at the Earth Resources Observation and Science (EROS) center. To analyze vegetation density, we used Landsat 8 data from 2014-2015.

2.2 Remote Sensing Processing

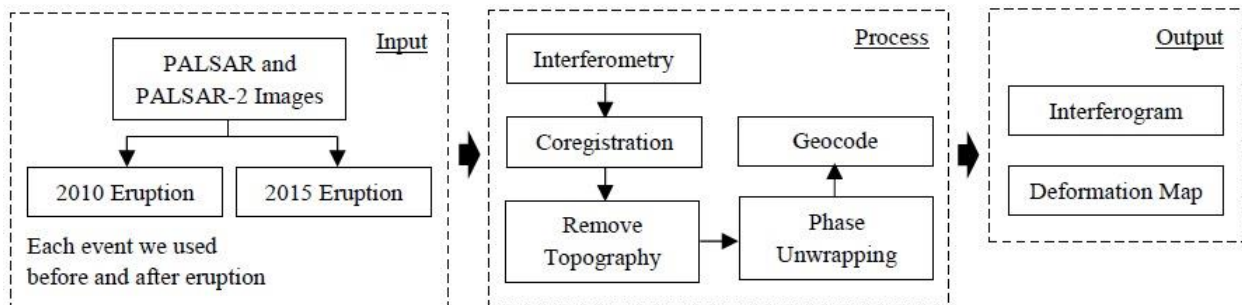


Figure 2. Flowchart Study

In this study we proposed InSAR method in the conventional single-interferogram approach, exploits two radar images of the same area acquired at different times to measure ground displacement. The technique uses the phase difference of backscattered signals from the two acquisitions to measure differential motion in the Line of Sight (LOS) direction include vertical and horizontal components. The InSAR deformation image produced from two SAR images that associated the 2010 and 2015 eruptions.

To measure ground deformation with high spatial resolution and accuracy on the large area observation we used differential synthetic aperture radar interferometry (Massonet 2008; Gabriel A K et al, 1989) which phase can be subtracted from the SAR interferogram to remove topography. DInSAR used to analysis the line of sight displacement for monitoring and detecting change volcano in long-term and short-term (Papageorgiou, E et al, 2012) and also for studying fault mechanism (Currenti G et al, 2010). We presented the interferometric analysis using snap software, a common architecture for all Sentinel Toolboxes is being jointly developed by Brockmann Consult, Array Systems computing and C-S called Sentinel Application Platform by ESA, (2016) to get interferogram and line of sight displacements, the interferometric phase was unwrapped with the SNAPHU program.

2.3 Normalized Difference Vegetation Index (NDVI)

Normalized Difference Vegetation Index (NDVI) is one of the best indices for evaluating crop health and NIR sensors are necessary to measure it. NDVI mathematically compares red and NIR light signals to help differentiate plant from non-plant and healthy plant from sick plant. NIR sensors and drone software make it simple for agronomists and farmers to benefit from NDVI by creating maps that convert the ratios of invisible NIR light into colors humans can see and quickly. We use the algorithm such as :

$$NDVI = \frac{(NIR - Red)}{(NIR + Red)} \quad \text{Landsat 8 :} \quad NDVI = \frac{\text{Band 5} - \text{Band 4}}{\text{Band 5} + \text{Band 4}}$$

3. RESULT AND DISCUSSION

3.1 Ground Deformation

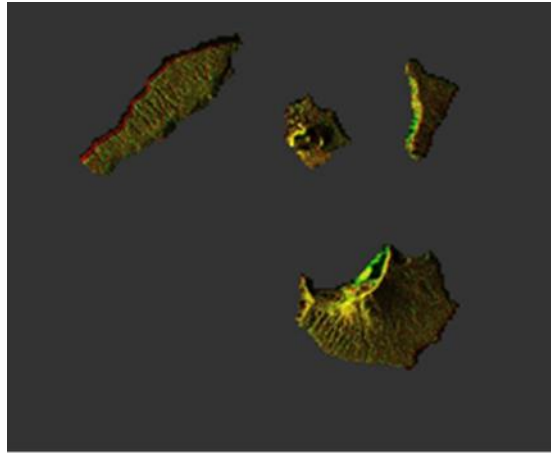


Figure 2. Images from the shape of area is made by coregistration of SLC images between slave and master images, take in different time.

For The RGB View can be useful for amplitude change detection. Regarding to ESA SNAP (2016) those images, we will see things that have changed in red or green and things that have not changed in yellow. It is also a visual indication that the coregistration has properly aligned both images. The resulting of RGB view should look mostly yellow. Poor registrations will have badly lined up terrain. The first result of interferograms as RGB could be allowed us to study interferometric SAR in volcano disaster.

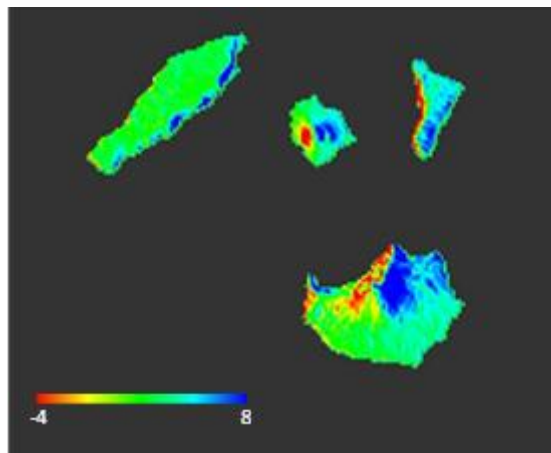


Figure 3. The image of displacement results of Krakatoa with the color range unit of centimeters.

Due to periodic eruptions, the growth of the young cone becomes larger and conceals the old cone. The figure 2 shows the body over Mt. Anak Krakatoa becomes bigger, but there is no correlation among the complex of Krakatoa to explain the connectivity of each part about the complex of mountain growth.

Based on CVGHM Indonesia, Anak Krakatoa is a typical cinder cone with an approximate radius of 2 km. It rises up to 315 m above sea level and shows ongoing moderate activity, having grown at an average rate of ~8 cm/week over the last 80 years. In the area of Java and Sumatra, the northward subduction of the Indian oceanic plate under the Sunda block occurs at a rate of about 6.8–7.2 cm/yr [DeMets et al., 1990]. The displacement over Mt. Anak Krakatoa is relatively massive this could be affected by activity which dominated by continuing tremor vibration with maximum amplitude which tend to fluctuate with a potential to evoke freatik eruptions and magmatic materials. The evidences can be taken to control potential geohazard is possible to be obtained.

3.2 Local Seismic Tomography

Following this study, we used the results of SAR interferometry and then we compared with local tomography observations to get better correlation among the satelllite image data and land observations data over the complex of Krakatoa. Jaxybulatov (2011) has pointed out of tomographic model with the distribution of P and S velocities and V_p / V_s ratio using local seismicity data and will explain in details in figure 3. Based on the results, the research found indications for a multilayered structure of a magma chamber system beneath the Krakatoa complex which seems to be in petrological studies (mineralmelt equilibria). The volcano is located just above the seismicity cluster at 150 km depth, and the low-velocity pattern which links the cluster with the caldera is vertical. The case of Krakatoa appears to be similar to that of Toba: the seismicity is shifted laterally to only ~ 20 km in respect to the volcano complex

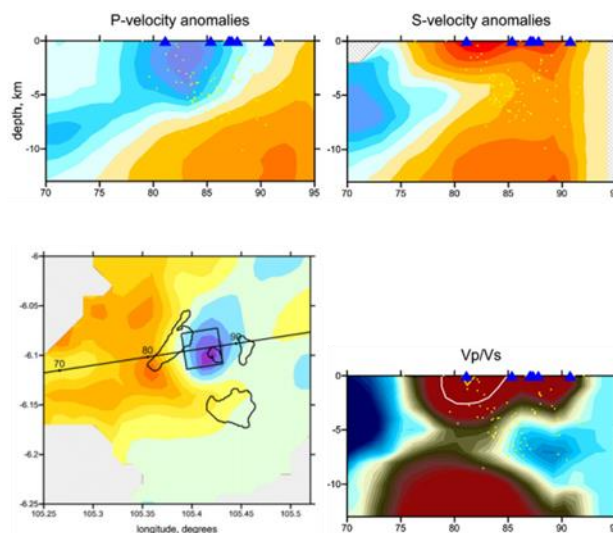


Figure 4. Vertical sections of the distributions of P and S anomalies (modified from Jaxybulatov, 2016).

In figure 3, the calculation using Vp-Vs inversion scheme and Vp/Vs ratio (calculated using Vp-Vp/Vs inversion scheme), obtained from real data inversion. Location of the profile is indicated in Fig. 3. Blue triangles: seismic stations. Yellow dots: final locations of the sources. Zones of anomalously high Vp/Vs ratios are indicated by the white contour line. A large negative anomaly located to the SW of the Krakatoa complex with the amplitude of -6% for P- and S-anomalies. This anomaly strongly affects the travel time of the rays from events located inside. It can be seen that P and S anomalies are resolved much less robustly than Vp/Vs patterns.

3.3 Vegetation Density

The mountain vegetation density of anak Krakatoa in 2014-2015 such as Table 1.

Table 1 Vegetation Density of anak Krakatoa in 2014-2015

Year	Classification of NDVI (pixels)			NDVI Difference (pixels)		
	Low	Medium	Height	Low	Medium	Height
2015	4418	70	553	16	11	27
2014	4402	59	580			

From 2014 to 2015 the vegetation density in Gunung Anak Krakatoa was based on the classification from the forestry department in 2003 which experienced the highest difference, namely high class with a high vegetation density of 27 pixels.

CONCLUSION

We found the growth of the young cone becomes larger and conceals the old cone. To find out the subsurface structure, a seismic tomography study was conducted using micro earthquake from the volcanic process itself. To get more details of result, comparison among the data is a necessary to interpretate the distribution of magma chambers beneath the Krakatoa complex. Location of the caldera and the active Anak Krakatoa is schematically created from the result of the distribution of Vp/Vs ratio in the vertical section.

REFERENCES

Cumming, I.G., et al. 2005. Digital Processing of Synthetic Aperture Radar Data. Artech House Remote Sensing Library.

DLR. 2014. Module 2201: SAR Interferometry Basics. https://saredu.dlr.de//unit/insar_basics. Diakses pada tanggal 13 Maret 2017.

Jaxybulatov, K. et al. 2016. Seismic anisotropy reveals a large magmatic sill complex below the Toba caldera. *Science* 346, 617–619.

Massonnet, D. and Rabaute, T., 1993. Radar interferometry: limits and potential. *IEEE Transactions on Geoscience and Remote Sensing*, 31(2), pp.455-464

BIOGRAPHICAL NOTES

CONTACTS

Dzauqi Arani
Indonesian Surveyor Association

Nine Residence Apartment, Pancoran, South Jakarta
Jakarta
Indonesia
+62 812 80281 172
dzauqi.arani18@gmail.com

Investigating Ground Deformation at Krakatoa Volcano Derived From InSar and Local Seismic Tomography Analysis (10615)

Dzauqi Arani, Mutiara Jamilah, Daffa Arrofi, Arliandy Arbad and Lucky Fakhriadi (Indonesia)

FIG Working Week 2020

Smart surveyors for land and water management

Amsterdam, the Netherlands, 10-14 May 2020